

## Interaction of *p*-cymene with $\beta$ -cyclodextrin

M. R. Serafini · P. P. Menezes · L. P. Costa · C. M. Lima · L. J. Quintans Jr ·  
J. C. Cardoso · J. R. Matos · J. L. Soares-Sobrinho · S. Grangeiro Jr ·  
P. S. Nunes · L. R. Bonjadim · A. A. S. Araújo

Received: 27 April 2011 / Accepted: 7 June 2011 / Published online: 17 July 2011  
© Akadémiai Kiadó, Budapest, Hungary 2011

**Abstract** In this investigation, the study of inclusion complexes formation between *p*-cymene and  $\beta$ -cyclodextrin using the methods of physical mixture, paste (PC) and slurry (SC), was evaluated. The results of DSC and TG/DTG showed that the products prepared by PC and SC methods were able to incorporate greater amounts of *p*-cymene, as evidenced by the weight loss of 7.15 and 3.97%, respectively, which occurred between 120 and 270 °C. SEM images showed decreased size of the household, especially in the SC product. The absorption bands in the IR spectrum, characteristic of *p*-cymene, were also identified in the preparations, indicating the presence of the compound in the complex.

**Keywords** *p*-cymene ·  $\beta$ -cyclodextrin ·  
Inclusion complexes

### Introduction

The importance of *p*-cymene is due to its utilization as an intermediate in the industrial fine chemicals syntheses for fragrances, flavorings, herbicides, pharmaceuticals, *p*-cresol production, syntheses of not nitrated musk's (i.e., tonalide), etc [1]. Furthermore, *p*-cymene is present in volatile oils from over 100 plants and occurs naturally in more than 200 foods (orange juice, grapefruit, tangerine, carrots, raspberries, butter, nutmeg, oregano, and almost every spice). *p*-cymene is not a terpene but is frequently encountered in terpene hydrocarbon chemistry, as a result of the oxidation or re-arrangement of mono-terpene hydrocarbons (C<sub>10</sub>H<sub>16</sub>). Terpenes and *p*-cymene are released into the atmosphere by plants [2].

The host–guest complexes of pharmaceutical compounds with cyclodextrins (CDs) have, therefore, been extensively studied and utilized to improve their solubility, dissolution rate, and bioavailability of poorly water-soluble drugs [3, 4]. CDs are donut-shaped cyclic oligosaccharides composed of six ( $\alpha$ ), seven ( $\beta$ ), and eight ( $\gamma$ ) glucopyranose units linked by  $\alpha$ -(1,4) linkages. The exterior of the CDs is highly hydrophilic due to the presence of numerous hydroxyl groups while the cavity in the interior of the CDs is hydrophobic and, thus, interacts with a variety of hydrophobic compounds to form inclusion complexes [5–7]. The size and shape of the torus-shaped hydrophobic cavity in combination with the size, polarity, and polarizability of the guest are major determinants for the formation of inclusion complexes [8–10].

CD can increase the aqueous solubility, chemical reactivity, and spectral properties of numerous lipophilic drugs which are used as guest molecules, without changing their intrinsic ability to permeate lipophilic membranes. Of these host molecules,  $\beta$ -CD is widely employed to enhance the

---

M. R. Serafini · P. P. Menezes ·  
L. J. Quintans Jr · S. Grangeiro Jr · P. S. Nunes ·  
L. R. Bonjadim · A. A. S. Araújo (✉)  
Departamento de Fisiologia, Universidade Federal de Sergipe,  
Av. Marechal Rondon, s/n, Cidade Universitária, São Cristóvão,  
SE CEP 49100-000, Brazil  
e-mail: left.ufs@hotmail.com

L. P. Costa · C. M. Lima · J. C. Cardoso  
Instituto de Tecnologia e Pesquisa da Universidade Tiradentes-  
ITP/UNIT, Av. Murilo Dantas, 300, Aracaju, SE CEP  
49032-490, Brazil

J. R. Matos  
Departamento de Química Fundamental, Instituto de Química,  
Universidade de São Paulo, Av. Lineu Prestes, 748, São Paulo,  
SP 05508-000, Brazil

J. L. Soares-Sobrinho  
Departamento de Química, Universidade Federal de Sergipe,  
Av. Marechal Rondon, s/n, Cidade Universitária, São Cristóvão,  
SE CEP 49100-000, Brazil

solubility, stability, and bioavailability of drugs and is the preferred agent for encapsulation of drugs in the pharmaceutical industry, because of its low price and high rate of production [3, 4, 9, 11]. Other applications of CD complexes with pharmaceuticals include elimination of undesirable drug properties, such as irritation and unpleasant odor or taste and improved stability of light and oxygen sensitive drugs [8, 10].

In the present study, it seemed of interest to investigate the complexation of *p*-cymene with  $\beta$ -CD. To this aim, *p*-cymene/ $\beta$ -CD combinations were prepared using different methods under controlled experimental conditions. Slurry (SC) and paste (PC) methods [12] were employed to prepare solid *p*-cymene/ $\beta$ -CD complexes, and their properties were compared with pure *p*-cymene,  $\beta$ -CD, and *p*-cymene/ $\beta$ -CD physical mixtures. The complexes were characterized by differential scanning calorimetry (DSC), thermogravimetry/derivative thermogravimetry (TG/DTG), and infrared spectroscopy (FTIR). The water content was determined by Karl Fischer titration. The complexes were also characterized regarding microstructure using scanning electron microscopy (SEM).

## Experimental

### Samples and preparation of inclusion complexes

1-methyl-4-(1-methylethyl)benzene or *p*-cymene was purchased from Sigma, USA (99.7%).  $\beta$ -CD (batch number 127K0753) was obtained from Sigma-Aldrich.

Inclusion complexes were prepared by three different procedures. A physical mixture (PM) was prepared by the addition of *p*-cymene to an agate mortar containing powdered  $\beta$ -CD under manual agitation. The *p*-cymene/ $\beta$ -CD 1:1 molar ratio was maintained as described for the inclusion complex preparation, and the mechanical mixture was stored in airtight glass containers.

Paste complexation (PC) was carried out by homogenization of  $\beta$ -CD (3.405 g) with water (1.2:4, v/w) directly in an agate mortar. In a second step, 402.6 mg of *p*-cymene (1:1 molar guest:host ratio) were added to  $\beta$ -CD paste under constant manual agitation. Then, the material was dried at room temperature (in a desiccator) till the formation of a glass film, which was removed by manual trituration and stored in airtight glass containers.

Slurry complexation (SC) was carried out by the addition of water to a beaker containing 3.405 g of  $\beta$ -CD (3:4, v/w). 402.6 milligrams of *p*-cymene, which is equal to about a 1:1 molar guest:host ratio, were added to the slurry and stirred for 40 min by a magnetic stirring device operating at 400 rpm (Quimis Q 261A21, Brazil). Thereafter,

the mixture was heated to 70 °C for 2 h in the same device, transferred to an agate mortar, and dried in a desiccator.

### Measurements

DSC curves were obtained in a DSC-50 cell (Shimadzu) using aluminum crucibles with about 2 mg of samples, under dynamic N<sub>2</sub> atmosphere (50 mL min<sup>-1</sup>) and heating rate of 10 °C min<sup>-1</sup> in the temperature range from 25 to 600 °C. The DSC cell was calibrated with indium (m.p. 156.6 °C;  $\Delta H_{\text{fus.}} = 28.54 \text{ J.g}^{-1}$ ) and zinc (m.p. 419.6 °C). TG/DTG curves were obtained with a thermobalance model TGA 50 (Shimadzu) in the temperature range 25–900 °C, using platinum crucibles with ~3 mg of samples, under dynamic N<sub>2</sub> atmosphere (50 mL min<sup>-1</sup>) and heating rate of 10 °C min<sup>-1</sup>.

Karl Fischer titration was carried out at 25 ± 1 °C with a Karl Fischer titrator Analyzer (Mettler® DL 18).

The infrared absorption spectra of pure *p*-cymene,  $\beta$ -CD, and *p*-cymene/ $\beta$ -CD complexes obtained by physical mixture, paste and slurry methods were obtained at room temperature in the range 4000–400 cm<sup>-1</sup> in KBr pellets using a Perkin–Elmer FTIR spectrophotometer.

The dried products were mounted on aluminum stubs, coated with a thin layer of gold and visualized with a JEOL Model JSM-6360-LV scanning electron microscope, at an accelerated voltage of 20 kV.

## Results and discussion

Different analytical techniques, such as DSC, TG/DTG, FTIR, and SEM, were employed to characterize and compare the physicochemical properties of the solid complexes prepared between *p*-cymene and  $\beta$ -CD, to investigate and compare the potential and effectiveness of the different preparation methods.

DSC curves of pure *p*-cymene,  $\beta$ -CD, and *p*-cymene/ $\beta$ -CD complexes obtained by physical mixture, paste and slurry methods are shown in Fig. 1. The *p*-cymene showed a sharp melting endotherm at 78.2 °C, this refers to volatilization of the compound. This event was also seen in the TG/DTG curve (Fig. 2), that represents mass loss of 99.02% in the range of 25–145 °C ( $T_{\text{peakDTG}} = 124.6 \text{ °C}$ ).

DSC curve of  $\beta$ -CD showed four events of 25–400 °C. The first event is related to the water releasing ( $T_{\text{peakDSC}} = 80.8 \text{ °C}$  e  $\Delta m_1 = 11.63\%$ ). With the no significant mass loss in the TG/DTG, the second event ( $T_{\text{peak}} = 216 \text{ °C}$ ) related the phase transition of  $\beta$ -CD. The others events are endothermic and exothermic assigned to thermal decomposition. TG/DTG curves showed thermal decomposition  $\beta$ -CD started above 270 °C and occurs with elemental carbon formation because of the sample

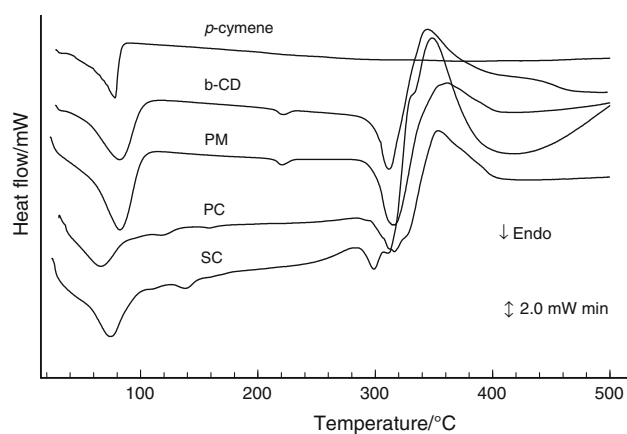


**Fig. 1** DSC curves of *p*-cimeno,  $\beta$ -CD, physical mixture (PM), paste complex (PC), and slurry complex (SC) in dynamic nitrogen atmosphere ( $100 \text{ mL min}^{-1}$ ) and hate heat  $10 \text{ }^\circ\text{C min}^{-1}$

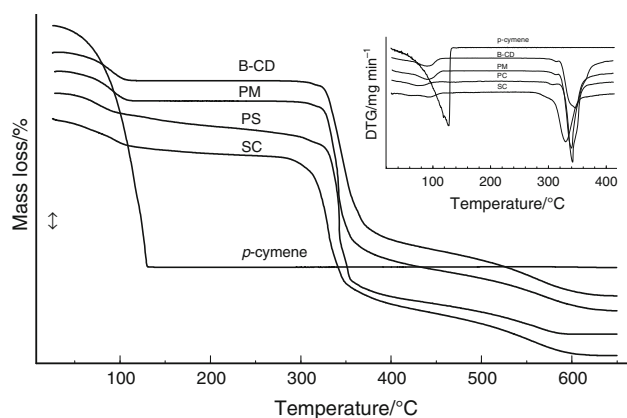


**Fig. 2** TG curves of *p*-cimeno,  $\beta$ -CD, physical mixture (PM), paste complex (PC), and slurry complex (SC) in dynamic nitrogen atmosphere ( $100 \text{ mL min}^{-1}$ ) and hate heat  $10 \text{ }^\circ\text{C min}^{-1}$

carbonization. Between 360 and  $900 \text{ }^\circ\text{C}$ , the elemental carbon is released slowly. Results were similar to  $\beta$ -CD obtained by Rodríguez-Tenreiro et al. [13] and Xu et al. [14].

Figure 2 shows the TG and DTG curves for the *p*-cimeno,  $\beta$ -CD, physical mixture (PM), paste complex (PC) and slurry complex (SC) and Table 1 lists the mass losses calculated from specific intervals for each material studied in the present work. The PM exhibits 12.11%, the paste (PC) 9.51%, and the slurry (SC) 11.46% of mass loss up to  $120 \text{ }^\circ\text{C}$  (Fig. 2). It can be attributed mainly to the water loss and to the release of a small amount of guest from the samples. Between 120 and  $270 \text{ }^\circ\text{C}$ , 0.28–7.15% further mass change was recorded which may be due to the release of the *p*-cymene (guest component) from their inclusion complexes. The curve of the PM was a superposition of the guest and host curves, which indicates a lower evidence of interaction. The curve of the complex prepared by slurry method (SC) showed a water/oil loss

**Table 1** Mass losses for *p*-cimeno,  $\beta$ -CD, physical mixture, and *p*-cimeno/ $\beta$ -CD complexes and moisture contents obtained by Karl Fisher method

	Mass loss/%				Karl Fisher % Water
	First step	Second step	Third step	Fourth step	
<i>p</i> -cymene	99.02 <sup>a</sup>	–	–	–	2.73
$\beta$ -CD	11.63 <sup>b</sup>	–	64.58 <sup>e</sup>	23.44 <sup>f</sup>	15.46
Physical mixture (PM)	12.11 <sup>c</sup>	0.28 <sup>d</sup>	62.42 <sup>e</sup>	23.18 <sup>f</sup>	15.37
Paste complex (PC)	9.51 <sup>c</sup>	7.15 <sup>d</sup>	64.38 <sup>e</sup>	17.69 <sup>f</sup>	10.77
Slurry complex (SC)	11.47 <sup>c</sup>	3.97 <sup>d</sup>	55.60 <sup>e</sup>	25.77 <sup>f</sup>	11.68

<sup>a</sup> Percentage of the *p*-cymene evaporates up to  $145 \text{ }^\circ\text{C}$

<sup>b</sup> Percentage of water releasing up to  $120 \text{ }^\circ\text{C}$

<sup>c</sup> Mass loss related to evaporation of the *p*-cymene and the water release up to  $120 \text{ }^\circ\text{C}$

<sup>d</sup> Mass loss probably attributed to *p*-cymene release in the interval from 120 to  $270 \text{ }^\circ\text{C}$

<sup>e</sup> Thermal decomposition in the interval from 270 to  $365 \text{ }^\circ\text{C}$

<sup>f</sup> Elemental carbon formation due to sample carbonization in the interval from 365 to  $900 \text{ }^\circ\text{C}$

event from r.t up to  $120 \text{ }^\circ\text{C}$ . In the interval from 120 to  $270 \text{ }^\circ\text{C}$ , a gradual mass loss (3.97%) was recorded and can be attributed to *p*-cymene. On the other hand, the curve of the complex prepared by paste method (PC) was similar to the SC curve, but showed an important difference between 120 and  $270 \text{ }^\circ\text{C}$ . In this interval, the PC curve presents an acute mass loss event, which gives a strong indication of guest inclusion, in contrast to that observed by SC. This data is corroborating with DSC analyze. For this method, between 120 and  $270 \text{ }^\circ\text{C}$ , 3.18% further mass loss was detected due to the release of oil from its inclusion complex. The complexation ratio can be attributed to the selected way of preparation (i.e., a part of the oil remained in the solution and/or some evaporation loss took place during the long complexation process) [15].

Table 1 shows the percentages of water calculated by Karl Fisher method and TG/DTG. It is important to note that TG cannot distinguish between the oil and water mass losses from physical mixture or inclusion complexes. Thus, a volumetric water determination method (Karl Fisher) was employed to evaluate the increase or decrease in the amount of water. In this study, it was observed that there was a reduction of 4.69% of water content when compared with the  $\beta$ -CD and the PC. This difference can be explained as a result of the formation of the inclusion complex of  $\beta$ -CD with *p*-cymene. *p*-cymene as a guest molecule substitutes for the original water molecules in the cavity of  $\beta$ -CD.

According to the above reaction, inclusion complex formation may be confirmed by FTIR spectrum because bands resulting from the included part of the guest molecule are generally shifted or their intensities altered [16]. For the FTIR spectrum of  $\beta$ -CD, a broad band with a transmittance peak at  $3333\text{ cm}^{-1}$  was assigned to the symmetric and asymmetric O–H stretching due to the many intermolecular hydrogen bonds of  $\beta$ -CD. Another band in the range from  $2980$  to  $2840\text{ cm}^{-1}$  represented the symmetric and asymmetric stretching of the methylene groups. The absorption bands in the  $1275$ – $1200\text{ cm}^{-1}$  regions were asymmetric C–O–C stretching, and the ones in the range of  $1075$ – $1020\text{ cm}^{-1}$  were symmetric C–O–C stretching. In the observed spectra of the inclusion complexes, bands due to CD were prominent. However, some bands attributed to the guest molecules could also be observed, since intense broad bands due to CD often interfere with the observation of weak bands due to guest molecules.

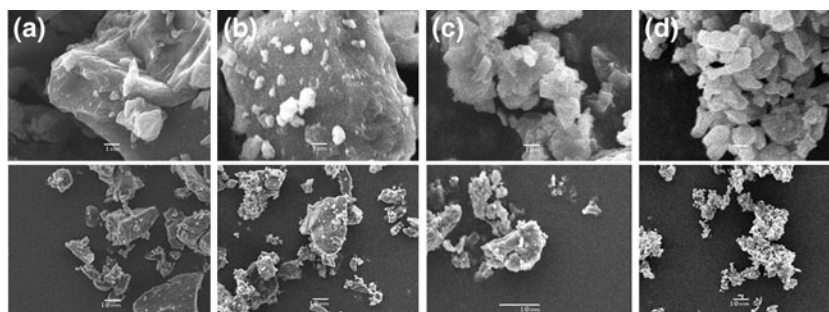
The *p*-cymene spectrum showed a =C–H stretches of aromatics ( $3099$ ,  $3068$ ,  $3032\text{ cm}^{-1}$ ) and the –C–H stretches of the alkyl (methyl) group ( $2925\text{ cm}^{-1}$ ). The characteristic overtones are seen from about  $2000$ – $1665\text{ cm}^{-1}$ . Also it is noted that the carbon–carbon stretches in the aromatic ring ( $1614$ ,  $1506$ ,  $1465\text{ cm}^{-1}$ ), and the in-plane C–H bending ( $1086$ ,  $1035\text{ cm}^{-1}$ ). IR spectrum of *p*-cymene exhibits also two bands at  $1363$  and  $1338\text{ cm}^{-1}$  assigned to isopropyl group. In the spectra of *p*-cymene/ $\beta$ -CD complexes obtained by PC and SC, similar bands as those of the *p*-cymene are observed, indicating that the complex formation did not affect the stability of the drug. The bands of *p*-cymene at  $1363$  and  $1678\text{ cm}^{-1}$  were shifted to  $1377$  and  $1644\text{ cm}^{-1}$  (for *p*-cymene/ $\beta$ -CD complexes obtained by SC) and  $1378$  and  $1631\text{ cm}^{-1}$  (PC). These changes may be related to the formation of intra-molecular hydrogen bonds between *p*-cymene and  $\beta$ -CD.

The scanning electron microscopy of  $\beta$ -CD and *p*-cymene/ $\beta$ -CD complexes obtained by physical mixing, paste and slurry methods are shown in Fig. 3. First, we observed powdered form of  $\beta$ -CD by SEM, and then we also observed powdered form of inclusion complex (Fig. 3).

$\beta$ -CD shows plated/sheeted structure and the solid inclusion complex structure is different from  $\beta$ -CD.  $\beta$ -CD consisted of irregularly shaped crystals (Fig. 3a). SEM pictures showed that the shape and size of the inclusion complexes were completely different from the ones of free  $\beta$ -CD or inclusion complexes. At the two methods (PC and SC) of the *p*-cymene/ $\beta$ -CD inclusion complexes studied, a compact and homogeneous powder-like structure was observed, Fig. 3c, d, the dimensions of which were smaller than those of the crystals of  $\beta$ -CD alone. The physical mixtures of *p*-cymene and  $\beta$ -CD powders revealed similarities with the  $\beta$ -CD free molecule (Fig. 3b), where residual  $\beta$ -CD crystals were easily identified (arrows). Pictures clearly elucidated the difference of powder of each other. Modification of crystal and powder can be assumed as a proof of the formation of new solid-inclusion complex (Fig. 3).

The formation of an inclusion complex can only be confirmed after the consideration of the results of several analytical approaches, such as phase solubility analysis, spectral methods, thermal analysis, and X-ray diffraction [17–19]. Marreto et al. [12], reported that the differences observed between inclusion ratios of the terpenes from both complexes can be attributed to differences between the formulation (water amount) and operational variables (temperature, type, and agitation time) used. Martin del Valle [20] reported that the water amount in complexation media needs to be enough to ensure an appropriate complexation rate that increases host and guest solubility, without excessively diluting these entities in the medium, which could prevent their contact at a sufficiently fast rate. Similarly, improvements in guest and host solubility can be achieved by increasing the temperature level, but heating, at the same time, can also destabilize the complex and contribute to losses of volatile guests by evaporation. Another relevant factor is oil dispersion in the medium. Oils in aqueous media have a tendency to associate with themselves rather than to interact with cyclodextrin. In these cases, good mixing allows better dispersion and a faster rate of complexation [20].

**Fig. 3** SEM micrographs of cross-sections (1 and  $10\text{ }\mu\text{m}$ ) of **a**  $\beta$ -CD, **b** physical mixture (PM), **c** paste complex (PC) and **d** slurry complex (SC)



## Conclusions

The results of this study clearly demonstrated that *p*-cymene could be efficiently complexed with  $\beta$ -CD to form an inclusion complex by the paste and slurry methods in a molar ratio of 1:1. The results of DSC, TG/DTG, SEM, and FTIR demonstrated that *p*-cymene/ $\beta$ -CD complex has different physicochemical characteristics from free *p*-cymene. In this study, paste method showed a better inclusion profile of the *p*-cymene when compared to slurry complexation. New studies by gas chromatography coupled to mass spectrometry (GC/MS) analysis are needed to evaluate the quantitative and qualitative assessment and comparison of the existing methods, and determined moisture, total oil, surface oil, and volatile profiles in the inclusion complex of  $\beta$ -CD and *p*-cymene.

**Acknowledgements** The authors would like to acknowledge the financial support provided by the Conselho Nacional de Desenvolvimento Científico e Tecnológico/CNPq/Brazil) and Fundação de Amparo à Pesquisa do Estado de Sergipe/FAPITEC-SE.

## References

1. Luengo MAM, Yates M, Domingo MJM, Casal B, Iglesias M, Esteban M, Ruiz-Hitzky E. Synthesis of *p*-cymene from limonene, a renewable feedstock. *Appl Catal B Environ*. 2008;81:218–24.
2. Philis JG. The S1  $\leftarrow$  S0 spectrum of jet-cooled *p*-cymene. *Spectrochim Acta Part A*. 2005;61:1239–41.
3. Abdoh AA, Zughul MB, Eric J, Davies D, Badwan AA. Inclusion complexation of diclofenac with natural and modified cyclodextrins explored through phase solubility,  $^1\text{H-NMR}$  and molecular modeling studies. *J Incl Phenom Macrocycl Chem*. 2007;57:503–10.
4. Ali H, Marzouqi A, Solieman A, Shehadi I, Adem A. Influence of the preparation method on the physicochemical properties of econazole- $\beta$ -cyclodextrin complexes. *J Incl Phenom Macrocycl Chem*. 2008;60:85–93.
5. Zielenkiewicz W, Kozbiał M, Golankiewicz B, Poznanski J. Enhancement of aqueous solubility of tricyclic acyclovir derivatives by their complexation with hydroxypropyl- $\beta$ -cyclodextrin. *J Therm Anal Calorim*. 2010;101:555–60.
6. Fernandes LP, Oliveira WP, Sztatiz J, Szilágyi IM, Cs. Novák. Solid state studies on molecular inclusions of *Lippia sidoides* essential oil obtained by spray drying. *J Therm Anal Calorim*. 2009;95(3):855–63.
7. Ambrus R, Aigner Z, Catenacci L, Bettinetti G, Szabo-Révész P, Sorrenti M. Physico-chemical characterization and dissolution properties of niflumonic acid-cyclodextrin-PVP ternary systems. *J Therm Anal Calorim*. 2011;104:291–7.
8. Ali SM, Upadhyay SK, Maheshwari A. NMR spectroscopic study of the inclusion complex of desloratadine with  $\beta$ -cyclodextrin in solution. *J Incl Phenom Macrocycl Chem*. 2007;59:351–5.
9. Salústio PJ, Feio G, Figueirinhas JL, Pinto JF, Marques HMC. The influence of the preparation methods on the inclusion of model drugs in a  $\beta$ -cyclodextrin cavity. *Eur J Pharm Biopharm*. 2009;71:377–86.
10. Marques HMC, Hadgraft J, Kellawat IW. Studies of cyclodextrin inclusion complexes. I. The salbutamol-cyclodextrin complex as studied by phase solubility and DSC. *Int J Pharm*. 1990;63:259–66.
11. Tsai Y, Tsai H, Wu C, Tsai F. Preparation, characterisation and activity of the inclusion complex of paeonol with  $\beta$ -cyclodextrin. *Food Chem*. 2010;120:837–41.
12. Marreto RN, Almeida EECV, Alves PB, Niculau ES, Nunes RS, Matos CRS, Araújo AAS. Thermal analysis and gas chromatography coupled mass spectrometry analyses of hydroxypropyl- $\beta$ -cyclodextrin inclusion complex containing *Lippia gracilis* essential oil. *Thermochim Acta*. 2008;475:53–8.
13. Rodríguez-Tenreiro C, Alvarez-Lorenzo C, Concheiro A, Torres-Labandeira JJ. Characterization of cyclodextrin-carbopol interactions by DSC and FTIR. *J Therm Anal Calorim*. 2004;77:403–11.
14. Xu P, Song LX, Wang HM. Study on thermal decomposition behavior of survived  $\beta$ -cyclodextrin in its inclusion complex of clove oil by nonisothermal thermogravimetry and gas chromatography coupled to time-of-flight mass spectrometry analyses. *Thermochim Acta*. 2008;469:36–42.
15. Martins AP, Craveiro AA, Machado MIL, Raffin FN, Moura TF, Novák Cs., Zsuzsanna Éhen J. Preparation and characterization of *Mentha  $\times$  villosa* Hudson oil- $\beta$ -cyclodextrin complex. *J Therm Anal Calorim* 2007;88:363–71.
16. Szente L. Analytical methods for cyclodextrins, cyclodextrin derivatives and cyclodextrin complexes. In: *Comprehensive supramolecular chemistry*, vol 3. Oxford: Pergamon Press; 1996. p. 253–78.
17. Nunes OS, Bezerra MS, Costa LP, Cardoso JC, Albuquerque RLC Jr, Rodrigues MO, Barin GB, Silva FA, Araújo AAS. Thermal characterization of usnic acid/collagen-based films. *J Therm Anal Calorim*. 2010;99:1011–4.
18. Cardoso JC, Albuquerque RLC Jr, Padilha FF, Bittencourt FO, Freitas O, Nunes PS, Pereira NL, Fonseca MJV, Araújo AAS. Effect of the Maillard reaction on properties of casein and casein films. *J Therm Anal Calorim*. 2011;104:249–54.
19. Brito MB, Barin GB, Araújo AAS, Sousa DP, Cavalcanti SCH, Lira AAM, Nunes RS. The action modes of *Lippia sidoides* (Cham) essential oil as penetration enhancers on snake skin. *J Therm Anal Calorim* 2009;97(1):323–7.
20. Martín Del Valle EM. Cyclodextrins and their uses: a review. *Process Biochem* 2004;39:1033–46.